Original Investigation

Time-Resolved Quantitative Analysis of the Diaphragms During Tidal Breathing in a Standing Position Using Dynamic Chest Radiography with a Flat Panel Detector System ("Dynamic X-Ray Phrenicography"): Initial Experience in 172 Volunteers

Yoshitake Yamada, MD, PhD, Masako Ueyama, MD, PhD, Takehiko Abe, MD, PhD, Tetsuro Araki, MD, PhD, Takayuki Abe, PhD, Mizuki Nishino, MD, MPH, Masahiro Jinzaki, MD, PhD, Hiroto Hatabu, MD, PhD, Shoji Kudoh, MD, PhD

Rationale and Objectives: Diaphragmatic motion in a standing position during tidal breathing remains unclear. The purpose of this observational study was to evaluate diaphragmatic motion during tidal breathing in a standing position in a health screening center cohort using dynamic chest radiography in association with participants' demographic characteristics.

Materials and Methods: One hundred seventy-two subjects (103 men; aged 56.3 ± 9.8 years) underwent sequential chest radiographs during tidal breathing using dynamic chest radiography with a flat panel detector system. We evaluated the excursions of and peak motion speeds of the diaphragms. Associations between the excursions and participants' demographics (gender, height, weight, body mass index [BMI], smoking history, tidal volume, vital capacity, and forced expiratory volume) were investigated.

Results: The average excursion of the left diaphragm (14.9 ± 4.6 mm, 95% CI 14.2–15.5 mm) was significantly larger than that of the right (11.0 ± 4.0 mm, 95% CI 10.4–11.6 mm) ($P < 0.001$). The peak motion speed of the left diaphragm (inspiratory, 16.6 ± 4.2 mm/s; expiratory, 13.7 ± 4.2 mm/s) was significantly faster than that of the right (inspiratory, 12.4 ± 4.4 mm/s; expiratory, 9.4 ± 3.8 mm/s) (both $P < 0.001$). Both simple and multiple regression models demonstrated that higher BMI and higher tidal volume were associated with increased excursions of the bilateral diaphragm (all $P < 0.05$).

Conclusions: The average excursions of the diaphragms are 11.0 mm (right) and 14.9 mm (left) during tidal breathing in a standing position. The diaphragmatic motion of the left is significantly larger and faster than that of the right. Higher BMI and tidal volume are associated with increased excursions of the bilateral diaphragm.

Key Words: Radiography; thorax; X-ray; respiration; diaphragm.

Acad Radiol 2016; ■:■■–■■

From the Department of Radiology, Center for Pulmonary Functional Imaging, Brigham and Women's Hospital, Harvard Medical School, 75 Francis St., Boston, MA 02215 (Y.Y., T.A., M.N., H.H.); Department of Diagnostic Radiology, Keio University School of Medicine, 35 Shinanomachi, Shinjuku-ku, Tokyo 160-8582 (Y.Y., M.J.); Department of Health Care, Fukujuji Hospital, Japan Anti-Tuberculosis Association, Kiyose, Tokyo (M.U.); Department of Radiology, Fukujuji Hospital, Japan Anti-Tuberculosis Association, Kiyose, Tokyo (T.A.); Department of Preventive Medicine and Public Health, Biostatistics Unit at Clinical and Translational Research Center, Keio University School of Medicine, Tokyo (T.A.); Department of Respiratory Medicine, Fukujuji Hospital, Japan Anti-Tuberculosis Association, Kiyose, Tokyo, Japan (S.K.). Received September 29, 2016; revised November 2, 2016; accepted November 2, 2016. **Address correspondence to:** Y.Y. e-mail: yamada@rad.med.keio.ac.jp; H.H. e-mail: hhatabu@partners.org

http://dx.doi.org/10.1016/j.acra.2016.11.014

INTRODUCTION

The bilateral diaphragm is the most important respiratory muscle. Diaphragmatic dysfunction is an underappreciated cause of respiratory difficulties and may be due to a wide variety of issues, including surgery, trauma, tumor, and infection (1). Several previous studies have evaluated diaphragmatic motion using fluoroscopy (2–5), ultrasound (6,7), magnetic resonance (MR) fluoroscopy (dynamic MR imaging [MRI]) (8–12), and computed tomography (CT) (13–16). However, the data of the previous studies using ultrasound, MR fluoroscopy, or CT were obtained in a supine position (6–16), not in a standing position. Also, while the data of the previous studies using fluoroscopy were obtained in a standing position, the data were assessed under forced breathing (2,3), not under tidal or resting breathing. Thus, diaphragmatic motion in a standing position during tidal breathing remains unclear, even though it is essential for understanding respiratory physiology in our daily life. Furthermore, the evaluation of diaphragmatic motion using fluoroscopy, ultrasound, dynamic MRI, or CT has not been used as a routine examination because of limitations, including high radiation dose, small field of view, low temporal resolution, and/or high cost.

Recently, dynamic chest radiography using a flat panel detector (FPD) system with a large field of view was introduced for clinical use. This technique can provide sequential chest radiographs with high temporal resolution during respiration (17), and the radiation dose is much lower than that of CT. Also, whereas CT and MRI are performed in the supine or prone position, dynamic chest radiology can be performed in a standing or sitting position, which is physiologically relevant. To the best of our knowledge, no detailed study has analyzed diaphragmatic motion during tidal breathing by using dynamic chest radiography.

The purpose of this study was to evaluate diaphragmatic motion during tidal breathing in a standing position in a health screening center cohort using dynamic chest radiography in association with participants' demographic characteristics.

MATERIALS AND METHODS

Study Population

This cross-sectional study was approved by the institutional review board, and all the participants provided written informed consent. From May 2013 to February 2014, consecutive 220 individuals who visited the health screening of our hospital and met the following inclusion criteria for the study were recruited: age greater than 20 years, scheduled for conventional chest radiography, and underwent pulmonary function test. Patients with any of the following criteria were excluded: pregnant ($n = 0$), potentially pregnant or lactating ($n = 0$), refused to provide informed consent ($n = 22$), had incomplete datasets of dynamic chest radiography ($n = 3$), had incomplete datasets of pulmonary function tests ($n = 1$), could not follow tidal breathing instructions (eg, holding breath or taking a deep breath) ($n = 18$), or their diaphragmatic motion could not be analyzed by the software described next ($n = 4$). Thus, a total of 172 participants (103 men, 69 women; mean age 56.3 ± 9.8 years; age range 36–85 years) were finally included in the analysis (Fig 1). The data from 47 participants of this study population were analyzed in a different study (under review). The heights and weights of the participants were measured, and the body mass index (BMI, weight in kilograms divided by height squared in meters) was calculated.

Imaging Protocol of Dynamic Chest Radiology ("Dynamic X-Ray Phrenicography")

Posteroanterior dynamic chest radiography ("dynamic X-ray phrenicography") was performed using a prototype system (Konica Minolta, Inc., Tokyo, Japan) composed of an FPD

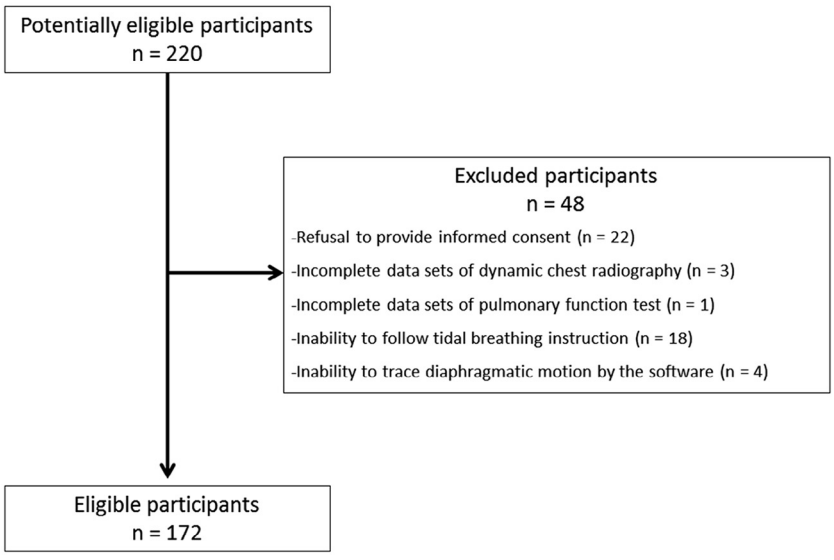

Figure 1. Flow diagram of the study population.

(PaxScan 4030CB, Varian Medical Systems, Inc., Salt Lake City, UT, USA) and a pulsed X-ray generator (DHF-155HII with Cineradiography option, Hitachi Medical Corporation, Tokyo, Japan). All participants were scanned in the standing position and instructed to breathe normally in a relaxed way without deep inspiration or expiration (tidal breathing). The exposure conditions were as follows: tube voltage, 100 kV; tube current, 50 mA; pulse duration of pulsed X-ray, 1.6 ms; source-to-image distance, 2 m; additional filter, 0.5 mm Al + 0.1 mm Cu. The additional filter was used to filter out soft X-rays. The exposure time was approximately 10–15 seconds. The pixel size was 388 × 388 μm, the matrix size was 1024 × 768, and the overall image area was 40 × 30 cm. The gray-level range of the images was 16,384 (14 bits), and the signal intensity was proportional to the incident exposure of the X-ray detector. The dynamic image data, captured at 15 frames/s, were synchronized with the pulsed X-ray. The pulsed X-ray prevented excessive radiation exposure to the subjects. The entrance surface dose was approximately 0.3–0.5 mGy.

Image Analysis

The diaphragmatic motions on sequential chest radiographs (dynamic image data) during tidal breathing were analyzed using prototype software (Konica Minolta, Inc.) installed in an independent workstation (Operating system: Windows 7 Pro SP1; Microsoft, Redmond WA; CPU: Intel Core i5-5200U, 2.20 GHz; memory 16 GB). The edges of the diaphragms on each dynamic chest radiograph were automatically determined by means of edge detection using a Prewitt Filter (18,19). A board-certified radiologist with 14 years of experience in interpreting chest radiography selected the highest point of each diaphragm as the point of interest on the radiograph of the resting end-expiratory position (Fig 2a). These points were automatically traced by the template-matching technique throughout the respiratory phase (Fig 2b, Supplementary Video S1), and the vertical excursions of the bilateral diaphragm were calculated (Fig 2c): the null point was set at the end of the expiratory phase, that is, the lowest point (0 mm) of the excursion on the graph is the highest point of each diaphragm at the resting end-expiratory position. Then the peak motion speed of each diaphragm was calculated during inspiration and expiration by the differential method (Fig 2c). If several respiratory cycles were involved in the 10 to 15-second examination time, the averages of the measurements were calculated.

Pulmonary Function Tests

The pulmonary function tests were performed in all participants on the same day of the imaging study. Parameters of pulmonary function tests were measured according to the American Thoracic Society guidelines (20,21) using a pulmonary function instrument with computer processing (DISCOM-21 FX, Chest MI Co, Tokyo, Japan).

Statistical Analysis

Descriptive statistics are expressed as mean ± standard deviation for continuous variables and as frequency and percentages for nominal variables. A paired *t* test was used to compare the excursion and peak motion speed between the right diaphragm and the left diaphragm. The associations between the excursions of the diaphragms and participants' characteristics were evaluated by means of the Pearson's correlation coefficient and a simple linear regression or Student's *t* test depending on the type of variable (ie, continuous or nominal variable). Continuous variables were height, weight, BMI, tidal volume, vital capacity (VC, %VC), forced expiratory volume (FEV_1, FEV_1%, and %FEV_1), and nominal variables were gender and smoking history. The robustness of the results of the univariate analyses was assessed with multiple linear regression models. The significance level for all tests was 5% (two sided). All data were analyzed using a commercially available software program (JMP; version 12, SAS, Cary, NC, USA).

RESULTS

Participants' Characteristics

Table 1 shows the clinical characteristics of all the participants ($n = 172$).

Excursions and Peak Motion Speeds of the Bilateral Diaphragm

The average excursion of the left diaphragm (14.9 mm ± 4.6 mm, 95% confidence interval [CI] 14.2 to 15.5 mm) was significantly larger than that of the right diaphragm (11.0 mm ± 4.0 mm, 95% CI 10.4 to 11.6 mm) ($P < 0.001$) (Table 2). The average peak motion speed of the left diaphragm (inspiratory: 16.6 ± 4.2 mm/s, 95% CI 16.0 to 17.2 mm/s; expiratory: 13.7 ± 4.2 mm/s, 95% CI 13.0 to 14.3 mm/s) was significantly faster than that of the right diaphragm (inspiratory: 12.4 ± 4.4 mm/s, 95% CI 11.8 to 13.1 mm/s; expiratory: 9.4 ± 3.8 mm/s, 95% CI 8.6 to 10.0 mm/s) (both $P < 0.001$) (Table 2).

Univariate Analysis of Associations Between the Diaphragmatic Excursions and Participants' Demographics

The results of univariate analyses of associations between the excursions and participant demographics are shown in Table 3. Higher BMI was associated with increased excursions of the bilateral diaphragm (right, $r = 0.25$, $P = 0.001$, 95% CI 0.10 to 0.39; left, $r = 0.28$, $P < 0.001$, 95% CI 0.14 to 0.42) (Fig 3a and 3b). Higher tidal volume was associated with increased excursions of the bilateral diaphragm (right, $r = 0.20$, $P = 0.008$, 95% CI 0.05 to 0.34; left, $r = 0.23$, $P = 0.003$, 95% CI 0.08 to 0.36) (Fig 3c and 3d). Higher age was associated with a decrease in the excursion of the right diaphragm ($r = -0.18$, $P = 0.017$, 95% CI −0.32 to −0.03). Higher weight was

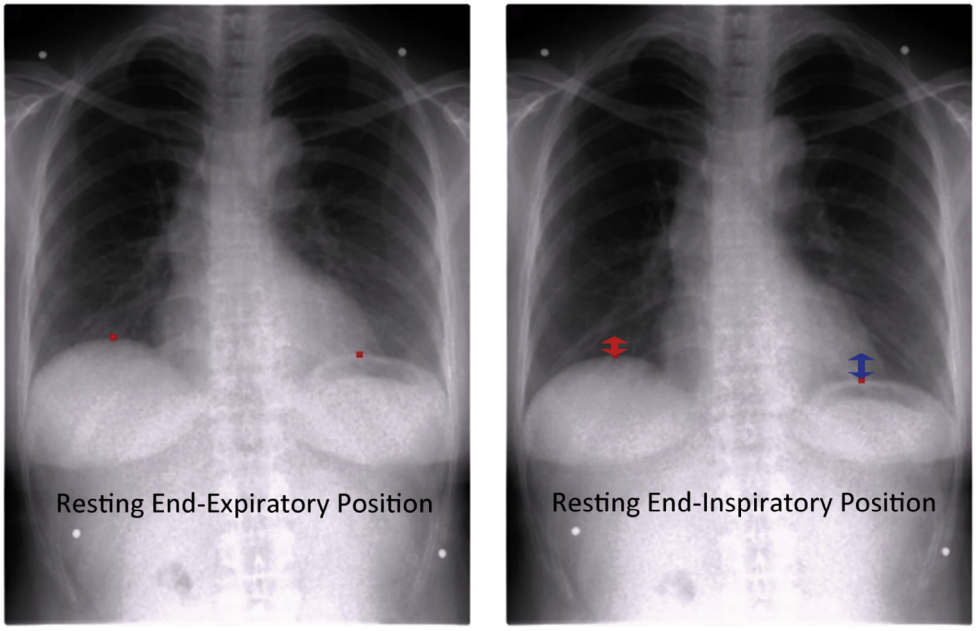

(a) (b)

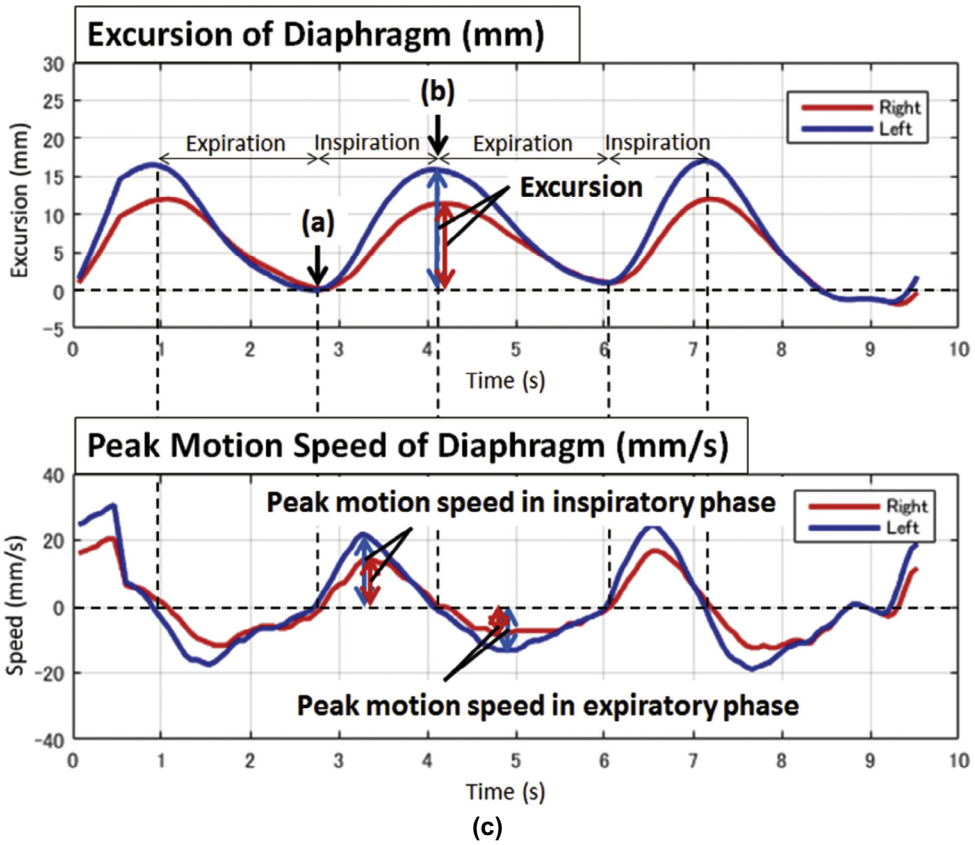

(c)

Figure 2. Representative sequential chest radiographs and the graphs of excursion and peak motion of the diaphragms obtained by chest dynamic radiography ("dynamic X-ray phrenicography"). **(a)** Radiograph of the resting end-expiratory position. **(b)** Radiograph of the resting end-inspiratory position. **(c)** Graph showing the vertical excursions and the peak motion speeds of the bilateral diaphragm. A board-certified radiologist placed a point of interest (red point) on the highest point of each diaphragm on the radiograph at the resting end-expiratory position (**a**). These points were automatically traced by the template-matching technique throughout the respiratory phase (double arrows in **b**) (Supplementary Video S1); red double arrow indicates the vertical excursion of the right diaphragm and blue double arrow indicates that of the left diaphragm. Based on locations of the points on sequential radiographs, the vertical excursions and the peak motion speeds of the bilateral diaphragm were calculated **(c)**. The lowest point (0 mm) of the excursion on the graph indicated that the highest point of each diaphragm was at the resting end-expiratory position (ie, null point was set at the end-expiratory phase) (**c**). (Color version of figure is available online.)

TABLE 1. Demographic Characteristics of the Study Population (172 Volunteers)

Demographic Variables	Value	
	Mean ± SD or *n* (%)	Range
Age (years)	56.3 ± 9.8	36–85
Female/Male (n, %)	69 (40.1)/103 (59.9)	—
Height (cm)	163.7 ± 9.0	137.9–184.2
Weight (kg)	61.0 ± 12.0	28.8–111.8
BMI (kg/m^2)	22.7 ± 3.2	15.1–37.7
Smoking history		
Current or Former	58 (33.7)	—
Never	114 (66.3)	—
Pulmonary function test		
Tidal volume (L)	0.76 ± 0.38	0.22–2.30
VC (L)	3.42 ± 0.83	1.24–5.70
%VC	107.7 ± 15.3	58.7–159.6
FEV_1 (L)	2.70 ± 0.68	1.06–4.72
FEV_1 %	80.8 ± 6.4	57.3–97.3
$\%FEV_1$	104.0 ± 14.9	55.1–163.9

BMI, body mass index; FEV, forced expiratory volume; SD, standard deviation; VC, vital capacity.
Range indicates the minimum–maximum.

associated with an increased excursion of the left diaphragm ($r = 0.22$, $P = 0.004$, 95% CI 0.07 to 0.36). Gender, height, smoking history, VC, %VC, FEV_1, FEV_1%, and $\%FEV_1$ were not associated with the excursions of the bilateral diaphragm (all $P > 0.05$).

Multivariate Analysis of Associations Between the Excursions and Participants' Demographics

Multiple linear regression analysis using all variables as factors (Model 1) demonstrated that weight, BMI, and tidal volume were independently associated with the bilateral excursion of the diaphragms (all $P < 0.05$) after adjusting for other clinical variables, including age, gender, smoking history, height, VC, %VC, FEV_1, FEV_1%, and $\%FEV_1$. There were no significant associations between the excursion of the diaphragms and variables including age, gender, smoking history, height, VC, %VC, FEV_1, FEV_1%, and $\%FEV_1$ (Table 4). Additionally, a multiple linear regression model using age, gender, BMI, tidal volume, VC, FEV_1, and smoking history as factors (Model 2) was also fit as a sensitivity analysis, taking into account the correlation among variables (eg, BMI, height, and weight; VC and %VC; FEV_1, FEV_1%, and $\%FEV_1$). Model 2 (Supplementary Data S1) gave results consistent with Model 1 (Table 4): higher BMI and higher tidal volume were independently associated with the increased bilateral excursion of the diaphragms (all $P < 0.05$). The adjusted R^2 in Model 1 was numerically higher than that in Model 2 (right, 0.19 vs. 0.16, respectively; left, 0.16 vs. 0.13, respectively).

DISCUSSION

Our study determined the average excursion of the diaphragms during tidal breathing in a standing position in a health screening center cohort using dynamic chest radiography ("dynamic X-ray phrenicography"). These findings are important because they provide reference values of diaphragmatic motion during tidal breathing useful for the diagnosis of diseases related to respiratory kinetics. Our study also suggests that dynamic X-ray phrenicography is a useful method for the quantitative evaluation of diaphragmatic motion with a radiation dose comparable to conventional posteroanterior chest radiography (22).

Our study demonstrated that the average excursions of the bilateral diaphragm during tidal breathing (right: 11.0 mm, 95% CI 10.4 to 11.6 mm; left: 14.9 mm, 95% CI 14.2 to 15.5 mm) were numerically less than those during forced breathing in previous studies using other modalities (2,7,8). Using fluoroscopy, Alexander reported that the average right excursion was 27.5 mm and the average left excursion was 31.5 mm during forced breathing in the standing position in 127 patients (2). Using ultrasound, Harris et al. reported that the average right diaphragm excursion was 48 mm during forced breathing in the supine position in 53 healthy adults (7). Using MR fluoroscopy, Gierada et al. reported that the average right excursion was 44 mm and the average left excursion was 42 mm during forced breathing in the supine position in 10 healthy volunteers (8). The difference in diaphragmatic excursion during tidal breathing versus forced breathing is unsurprising.

Our study showed that the excursion and peak motion speed of the left diaphragm are significantly greater and faster than

TABLE 2. Excursions and Peak Motion Speeds of the Bilateral Diaphragm During Tidal Breathing in a Standing Position (*n* = 172)

	Right	Left	Comparison Between Right and Left
	Mean ± SD (Range)	Mean ± SD (Range)	*P* Value*
Excursion of the diaphragm (mm)	11.0 ± 4.0 (2.2–23.7)	14.9 ± 4.6 (5.3–28.5)	<0.001
Peak motion speed of the diaphragm (inspiratory phase) (mm/s)	12.4 ± 4.4 (3.6–28.0)	16.6 ± 4.2 (6.3–27.7)	<0.001
Peak motion speed of the diaphragm (expiratory phase) (mm/s)	9.4 ± 3.8 (3.3–25.1)	13.7 ± 4.2 (5.1–26.2)	<0.001

* *P* values were calculated using paired *t* test.

TABLE 3. Univariate Analysis of Associations Between the Excursions and Participant Demographics (n = 172)

Demographic Variables	For Excursion of the Right Diaphragm		For Excursion of the Left Diaphragm	
Continuous Variables	r (95% CI)	P Value†	r (95% CI)	P Value†
Age (years)	–0.18 (–0.32 to –0.03)	0.017*	–0.11 (–0.26 to 0.04)	0.148
Height (cm)	–0.02 (–0.17 to 0.13)	0.752	0.10 (–0.05 to 0.24)	0.203
Weight (kg)	0.13 (–0.02 to 0.28)	0.084	0.22 (0.07 to 0.36)	0.004*
BMI	0.25 (0.10 to 0.39)	0.001*	0.28 (0.14 to 0.42)	<0.001*
Tidal volume	0.20 (0.05 to 0.34)	0.008*	0.23 (0.08 to 0.36)	0.003*
VC	0.00 (–0.15 to 0.15)	0.991	0.13 (–0.02 to 0.28)	0.084
%VC	0.00 (–0.15 to 0.15)	0.956	0.07 (–0.08 to 0.22)	0.348
FEV_1	–0.02 (–0.17 to 0.13)	0.807	0.12 (–0.03 to 0.26)	0.132
FEV_1%	–0.03 (–0.17 to 0.12)	0.738	–0.02 (–0.17 to 0.13)	0.757
%FEV_1	–0.13 (–0.28 to 0.02)	0.086	–0.02 (–0.17 to 0.13)	0.820
Nominal Variables	Difference (95% CI)	P Value‡	Difference (95% CI)	P Value‡
Gender	–0.60 (–1.84 to 0.64)	0.340	0.69 (–0.73 to 2.11)	0.340
Smoking history	–0.80 (–2.08 to 0.48)	0.222	0.00 (–1.47 to 1.47)	1.000

BMI, body mass index; CI, confidence interval; FEV, forced expiratory volume; VC, vital capacity.

* Indicates $P < 0.05$.

† P values were calculated using Pearson's correlation coefficient.

‡ P values were calculated using Student t test.

TABLE 4. Multivariate Analysis of Associations Between the Excursions and Participant Demographics Using All Variables as Factors (Model 1) (n = 172)

	For the Excursion of Right Diaphragm			For the Excursion of Left Diaphragm		
Variable	Coefficient†	SE	P Value‡	Coefficient†	SE	P Value‡
Intercept	–26.859	22.979	0.244	–36.777	26.818	0.172
Age	–0.053	0.118	0.652	–0.016	0.138	0.906
Gender	0.540	1.250	0.666	0.584	1.459	0.690
Height	0.163	0.157	0.301	0.229	0.184	0.214
Weight	–0.246	0.109	0.026*	–0.308	0.128	0.017*
BMI	0.949	0.302	0.002*	1.171	0.352	0.001*
Tidal volume	2.124	0.809	0.010*	2.205	0.944	0.021*
VC	2.588	3.625	0.476	2.356	4.231	0.578
%VC	0.014	0.106	0.899	–0.008	0.124	0.948
FEV_1	–3.257	4.675	0.487	–1.925	5.456	0.725
FEV_1%	0.106	0.102	0.304	0.059	0.119	0.624
%FEV_1	–0.039	0.113	0.731	–0.011	0.132	0.937
Smoking history	0.372	0.348	0.286	0.193	0.406	0.636

BMI, body mass index; FEV, forced expiratory volume; SE, standard error; VC, vital capacity.

Multiple linear regression analysis using all variables as factors demonstrates that weight, BMI, and tidal volume are independently associated with the bilateral excursion of the diaphragms after adjusting for other clinical variables including age, gender, smoking history, height, VC, %VC, FEV_1, FEV_1%, and %FEV_1.

* Indicates $P < 0.05$.

† Coefficient indicates increase in the dependent variable for one-unit increase in each independent variable.

‡ P values were calculated using multiple linear regression analysis.

those of the right. With regard to the excursion, the results of our study are consistent with those of previous reports using fluoroscopy in a standing position (2,3). However, in the previous studies evaluating diaphragmatic motion in the supine position, the asymmetric diaphragmatic motion was not mentioned (7,8). The asymmetric excursion of the bilateral diaphragm may be more apparent in the standing position, but may not be detectable or may disappear in the supine position. Although we cannot explain the reason for the asymmetry in diaphragmatic motion, we speculate that the

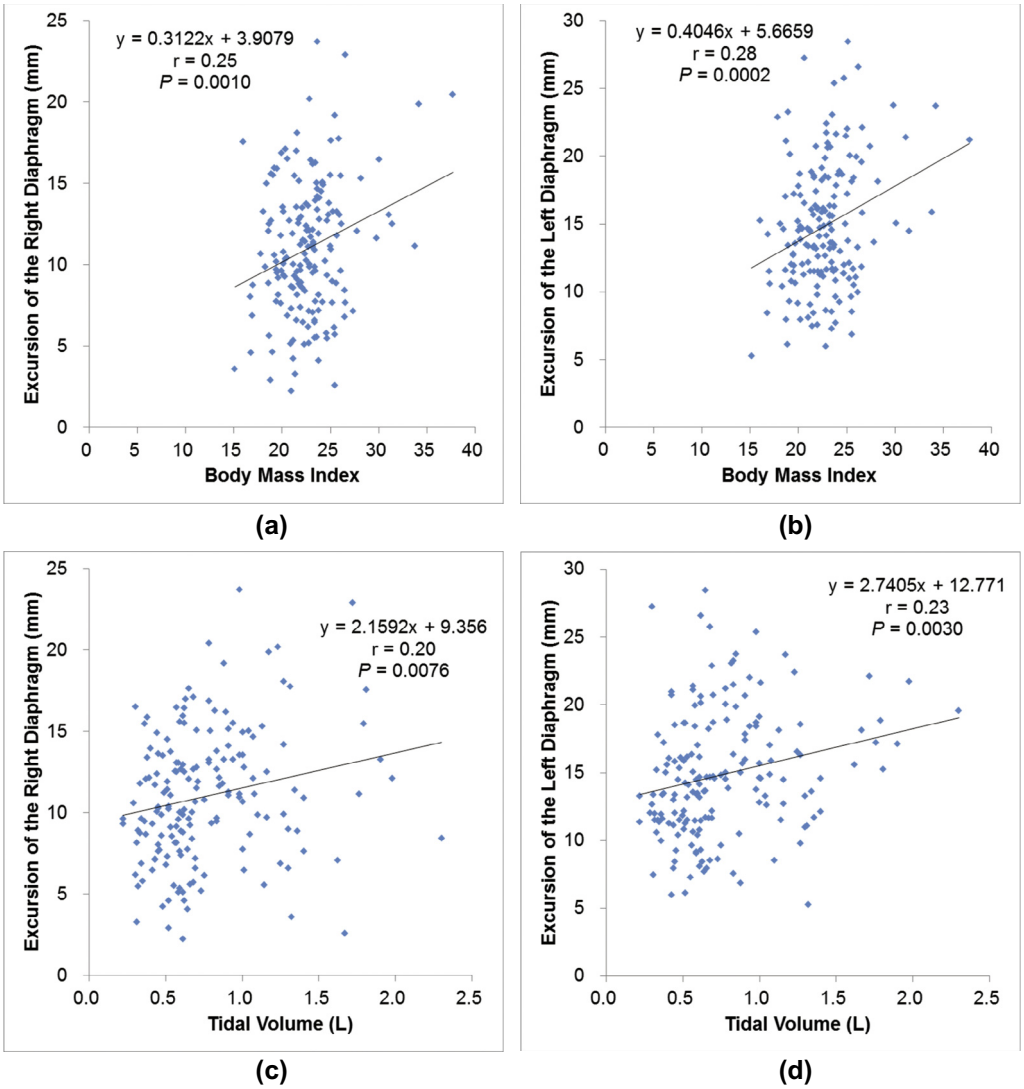

Figure 3. Estimated regression line of the excursion of the diaphragm on BMI or tidal volume. **(a)** Association between BMI and excursion of the right diaphragm. **(b)** Association between BMI and excursion of the left diaphragm. **(c)** Association between tidal volume and excursion of the right diaphragm. **(d)** Association between tidal volume and excursion of the left diaphragm. Lines show estimated regression **(a–d)**. All scatterplots show correlations ($P < 0.05$). BMI, body mass index.

presence of the liver may limit the excursion of the right diaphragm. Regarding the motion speed, to the best of our knowledge this study is the first to evaluate it. The faster motion speed of the left diaphragm compared to that of the right diaphragm would be related to the greater excursion of the left diaphragm.

We found that higher BMI and higher tidal volume were independently associated with the increased excursions of the bilateral diaphragm by both univariate and multivariate analyses, although the strength of these associations was weak. We cannot explain the exact reason for the correlation between BMI and the excursion of the diaphragm. However, a previous study showed that BMI is associated with peak oxygen consumption (23), and the increased oxygen consumption in an obese participant may affect diaphragmatic movement. Another possible reason is that lower thoracic compliance due to higher BMI may cause increased movement of the diaphragm for compensation. Regarding the correlation between tidal volume and excursion of the diaphragm, given that diaphragmatic muscle serves as the most important respiratory muscle, the result is to be expected. Considering our results, the excursion evaluated by dynamic X-ray phrenicography could potentially predict tidal volume.

Our study has several limitations. First, we included only 172 volunteers, and additional studies on larger participant populations are required to confirm these preliminary findings. Second, we evaluated only the motion of the highest point of the diaphragms for the sake of simplicity, and three-dimensional motion of the diaphragm could not be completely reflected in our results. However, we believe that this simple method would be practical and more easily applicable in a clinical setting.

CONCLUSIONS

The time-resolved quantitative analysis of the diaphragms with dynamic X-ray phrenicography is feasible. The average excursions of the diaphragms are 11.0 mm (right) and 14.9 mm (left) during tidal breathing in a standing position in our health screening center cohort. The diaphragmatic motion of the left is significantly larger and faster than that of the right. Higher tidal volume and BMI are associated with increased excursions of the bilateral diaphragm.

ACKNOWLEDGMENTS

The authors acknowledge the valuable assistance of Hideo Ogata, MD, PhD, Norihisa Motohashi, MD, PhD, Misako Aoki, MD, Yuka Sasaki, MD, PhD, and Hajime Goto, MD, PhD, from the Department of Respiratory Medicine; Yuji Shiraishi, MD, PhD, from the Department of Respiratory Surgery; and Masamitsu Ito, MD, PhD, Atsuko Kurosaki, MD, Yoichi Akiyama, RT, Kenta Amamiya, RT, and Kozo Hanai, RT, PhD, from the Department of Radiology, Fukujuji Hospital, for their important suggestions. The authors also acknowledge the valuable assistance of Alba Cid, MS, for editorial work on the manuscript. Yoshitake Yamada, MD, PhD, is a recipient of a research fellowship from the Uehara Memorial Foundation.

REFERENCES

1. Nason LK, Walker CM, McNeeley MF, et al. Imaging of the diaphragm: anatomy and function. Radiographics 2012; 32:E51–E70.
2. Alexander C. Diaphragm movements and the diagnosis of diaphragmatic paralysis. Clin Radiol 1966; 17:79–83.
3. Simon G, Bonnell J, Kazantzis G, et al. Some radiological observations on the range of movement of the diaphragm. Clin Radiol 1969; 20:231–233.
4. Verschakelen JA, Deschepper K, Jiang TX, et al. Diaphragmatic displacement measured by fluoroscopy and derived by Respitrace. J Appl Physiol 1989; 67:694–698.
5. Kleinman BS, Frey K, VanDrunen M, et al. Motion of the diaphragm in patients with chronic obstructive pulmonary disease while spontaneously breathing versus during positive pressure breathing after anesthesia and neuromuscular blockade. Anesthesiology 2002; 97:298–305.
6. Houston JG, Morris AD, Howie CA, et al. Technical report: quantitative assessment of diaphragmatic movement–a reproducible method using ultrasound. Clin Radiol 1992; 46:405–407.
7. Harris RS, Giovannetti M, Kim BK. Normal ventilatory movement of the right hemidiaphragm studied by ultrasonography and pneumotachography. Radiology 1983; 146:141–144.
8. Gierada DS, Curtin JJ, Erickson SJ, et al. Diaphragmatic motion: fast gradient-recalled-echo MR imaging in healthy subjects. Radiology 1995; 194:879–884.
9. Suga K, Tsukuda T, Awaya H, et al. Impaired respiratory mechanics in pulmonary emphysema: evaluation with dynamic breathing MRI. J Magn Reson Imaging 1999; 10:510–520.
10. Unal O, Arslan H, Uzun K, et al. Evaluation of diaphragmatic movement with MR fluoroscopy in chronic obstructive pulmonary disease. Clin Imaging 2000; 24:347–350.
11. Etlik O, Sakarya ME, Uzun K, et al. Demonstrating the effect of theophylline treatment on diaphragmatic movement in chronic obstructive pulmonary disease patients by MR-fluoroscopy. Eur J Radiol 2004; 51:150–154.
12. Iwasawa T, Takahashi H, Ogura T, et al. Influence of the distribution of emphysema on diaphragmatic motion in patients with chronic obstructive pulmonary disease. Jpn J Radiol 2011; 29:256–264.
13. Shirakawa T, Fukuda K, Miyamoto Y, et al. Parietal pleural invasion of lung masses: evaluation with CT performed during deep inspiration and expiration. Radiology 1994; 192:809–811.
14. Pettiaux N, Cassart M, Paiva M, et al. Three-dimensional reconstruction of human diaphragm with the use of spiral computed tomography. J Appl Physiol 1997; 82:998–1002.
15. Pan T, Lee TY, Rietzel E, et al. 4D-CT imaging of a volume influenced by respiratory motion on multi-slice CT. Med Phys 2004; 31:333–340.
16. Low DA, Nystrom M, Kalinin E, et al. A method for the reconstruction of four-dimensional synchronized CT scans acquired during free breathing. Med Phys 2003; 30:1254–1263.
17. Tanaka R, Sanada S, Okazaki N, et al. Evaluation of pulmonary function using breathing chest radiography with a dynamic flat panel detector: primary results in pulmonary diseases. Invest Radiol 2006; 41:735–745.
18. Prewitt JM. Object enhancement and extraction. In: Lipkin B, Rosenfeld A, eds. Picture processing and psychopictorics. New York: Academic, 1970; 75–149.
19. Wolffsohn JS, Mukhopadhyay D, Rubinstein M. Image enhancement of real-time television to benefit the visually impaired. Am J Ophthalmol 2007; 144:436–440.
20. Wanger J, Clausen JL, Coates A, et al. Standardisation of the measurement of lung volumes. Eur Respir J 2005; 26:511–522.
21. Miller MR, Hankinson J, Brusasco V, et al. Standardisation of spirometry. Eur Respir J 2005; 26:319–338.
22. IAEA. International basic safety standards for protection against ionizing radiation and for the safety of radiation sources. International Atomic Energy Agency Vienna, Safety Report Series No. 115, 1996.
23. Womack CJ, Hyman BA, Gardner AW. Prediction of peak oxygen consumption in patients with intermittent claudication. Angiology 1998; 49:591–598.

APPENDIX. SUPPLEMENTARY DATA

Supplementary data to this article can be found at http://dx.doi.org.10.1016/j.acra.2016.11.014.